ISSN 0020-4412, Instruments and Experimental Techniques, 2013, Vol. 56, No. 6, pp. 731–735. © Pleiades Publishing, Ltd., 2013.
Original Russian Text © S.V. Filatov, M.Yu. Brazhnikov, A.A. Levchenko, 2014, published in Pribory i Tekhnika Eksperimenta, 2014, No. 1, pp. 107–112.

LABORATORY TECHNIQUES

A Method for Spatial Recording of Waves on the Surface of a Transparent Liquid

S. V. Filatov*, M. Yu. Brazhnikov, and A. A. Levchenko

Institute of Solid State Physics, Russian Academy of Sciences,
ul. Akademika Osipyana 2, Chernogolovka, Moscow oblast, 142432 Russia
**e-mail: fillsv@issp.ac.ru*

Received December 14, 2012; in final form, September 3, 2013

Abstract—A method for recording standing waves on the surfaces of transparent liquids is proposed. A contrast pattern (grid) is placed on the bottom of a liquid-filled transparent cell and is photographed through a liquid layer in transmitted light. The shape of the vibrating liquid surface can be reconstructed from the distortions in the pattern image.

DOI: 10.1134/S0020441214010199

INTRODUCTION

At present, a number of techniques for studying capillary waves exist. Some of them are based on the registration of a refracted laser beam (LB) or an LB reflected from a comparatively small area of a liquid surface. For example, in [1], the shape of standing capillary waves on the surface of liquid hydrogen is evaluated from the change in the power of a reflected grazing LB. In [2], this technique is used to study nonlinear capillary waves on the ^{4}He surface.

In [3], waves on the surface of a conducting liquid were registered by inserting a vertically oriented segment of an insulated metal wire. As a result, a cylindrical capacitor is used, one of whose plates is the wire surface and the other plate is the conducting liquid. Oscillations of the liquid level at the contact point between the insulated wire and liquid can be evaluated by the time-dependent change in the capacitance of this capacitor.

The above-described techniques allow one to obtain information on the frequency distribution of the surface-vibration energy, but they cannot help to assess the energy distribution over wave vectors. In addition, the issues on the isotropy and uniformity of surface vibrations remain open-ended.

To measure the energy distribution over wave vectors on a liquid surface, the authors of [4, 5] photographed the surface of a semitransparent liquid that was illuminated from below. The diffuse light propagation in the liquid bulk was provided by introducing 1-μm-diameter polystyrene balls into the working cell with the liquid [4], and in the experiments performed in [5], ordinary milk was added to water. The brightness of individual points on a photograph of the vibrating surface is determined by the height of the liquid surface level; thus, the brightness distribution of points on the surface represents the energy (vibration amplitude) distribution over wave vectors on the surface of a "turbid" liquid that is illuminated from below. Note that adding fine-dispersed particles (polystyrene or fat balls floating in the liquid volume) to the liquid may have an effect on the properties of the studied liquid surface.

In [6], water-surface vibrations are excited by an electric field using the capacitive method. For this purpose, aluminum strips that serve as a capacitor are placed on a wall of the rectangular quartz cell. Waves are registered also using the capacitive method with the help of strips mounted on the other wall of the cell.

This paper describes a technique that is suitable for measuring the energy distribution over wave vectors in propagating and standing waves, which are excited on the surface of a transparent liquid. This technique is based on the computer processing of a series of photographs of a periodic grid, which lies on the bottom of a transparent cell, obtained through a vibrating transparent liquid (e.g., water) in transmitted light. Below, the measurement scheme, experimental-data processing algorithm, and results of studying the dispersion law for waves at frequencies of 10–400 Hz that were excited on the water surface in a rectangular cell with dimensions of 90 × 70 mm are presented.

TECHNIQUE FOR REGISTERING WAVES ON THE LIQUID SURFACE

If a thin film with a deposited contrast pattern is placed on the bottom of a liquid-filled flat transparent cell and the cell is illuminated from below, the pattern image on a photograph will be distorted if light is transmitted through the liquid–air interface. A schematic observation scheme is shown in Fig. 1. A camera records a distorted image of the pattern-periodic grid in the form of light spots against a dark background.

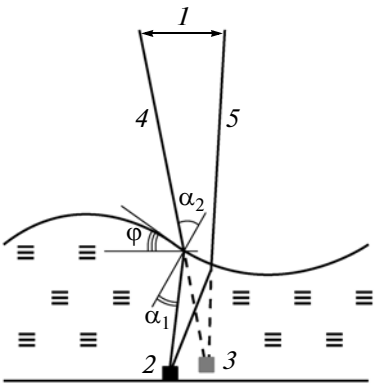

Fig. 1. Diagram of the observation scheme: (*1*) camera objective lens, (*2*) spot on the film, (*3*) image of the spot after the light transmission through the liquid surface, (*4*, *5*) light rays from a spot on the cell bottom to the camera objective lens, (φ) deflection angle of the liquid surface, (α_1) ray angle of incidence in the liquid, and (α_2) angle of the refracted ray in air.

Comparing a series of pattern photographs in the cases of a quiet and vibrating liquid surface allows reconstruction of the shape of surface vibrations.

A schematic diagram of the experimental setup is shown in Fig. 2. Support *1* with experimental cell *2*, which is filled with a liquid (water in this study), is installed on vibroplatform *7* (Mystery MO-10S subwoofer). The inner dimensions of the rectangular working cell are 90 × 70 mm, and the height of its collars is 10 mm. The bottom and collars of the cell are produced of chemical and organic glasses, respectively. A ГСПФ-053 sound generator is used to excite periodic vibrations of the vibroplatform. Film *5* on which a periodic grid of transparent spots against a dark nontransparent background is printed is positioned under the transparent bottom of cell *2*. The grid period is 250 μm, and the spot size is 50 μm. Digital camera *3* (Canon 50 D) is used to photograph the grid in visible light that passes through water layer *4*. The camera resolution is 4752 × 3168 pixels. The cell is illuminated with a Canon SpeedLite 580EX II pulse flash light (not shown in the figure). The light-pulse duration is 100 μs, which allows registering waves at frequencies of up to 1 kHz. Light from a photoflash is reflected from the dull surface of white sheet of paper *6* lying on stand *1*. The frame frequency in the operating mode is usually 0.10–0.05 s^{-1}, and the exposure duration is 20 times longer than the light-pulse duration.

Photographing was performed in an automatic mode: the camera and sound generator were controlled with the computer.

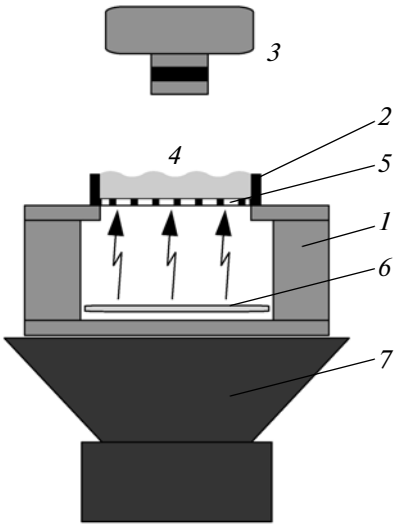

Fig. 2. Diagram of the experimental system: (*1*) support, (*2*) experimental cell, (*3*) digital camera, (*4*) water layer, (*5*) film with a periodic grid printed on it, (*6*) white sheet of paper, and (*7*) vibroplatform.

TECHNIQUE FOR PROCESSING PHOTOGRAPHS

To simplify calculations for reconstructing the shape of the vibrating liquid surface, each spot of the grid is considered as a point object on a photograph. The comparison of photographs of grid images in the cases of flat and vibrating surfaces allows one to draw a conclusion about the shape of the liquid surface at the shooting moment (Fig. 1).

Figure 3 shows fragments of photographs of the grid, which is positioned under the cell bottom and formed by transparent points against a black background. The photographing was performed through an 8-mm-high water layer with the unexcited (Fig. 3a) and excited (Fig. 3b) water surface. The vibroplatform was excited at a frequency of 37 Hz. The photograph shows that the distance between spots on the left is larger than that between spots on the right by a factor

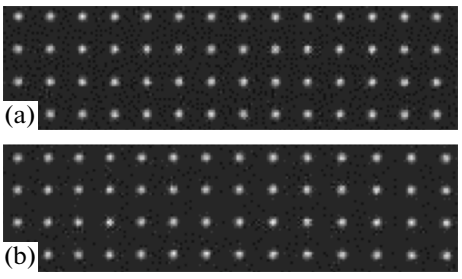

Fig. 3. Fragment of a grid photograph (a) through a quiet water layer and (b) through a water layer on whose surface waves are excited. The excitation frequency is 37 Hz and $A = 6$.

of ~1.2, thus indicating the presence of waves on the liquid surface.

The relationships between the surface shape and the position of spots on the photograph can be established using the light-refraction law at the interface of two optical media:

$$n_1 \sin\alpha_1 = n_2 \sin\alpha_2, \quad (1)$$

where n and α is the refractive index and the beam angle of incidence on the surface between the phases.

The displacement Δx on the grid photograph through the vibrating liquid surface relative to the spot position on the grid photograph through the stationary liquid surface depends on the depth d of the liquid layer, the surface tilt angle φ, and the ratio of the refractive indices n of the liquid at the phase interface:

$$\Delta x = d \sin\varphi_x \frac{1-n}{n}. \quad (2)$$

Under the assumption of small angles ($\varphi \ll 1$) formula (2) can be rewritten as

$$\Delta x \sim \varphi_x \sim \frac{\partial h}{\partial x}, \quad (3)$$

where $h(x, y)$ is the surface height at the point with the coordinates (x, y).

Similar reasoning is valid when describing the displacements of points along the Y axis. Thus, the displacement of spots on the grid photographs that were taken through the excited and unexcited liquid surfaces is proportional to the surface-height gradient:

$$\Delta \mathbf{r} \sim \nabla h. \quad (4)$$

EXPERIMENTAL DATA PROCESSING

As was mentioned above, Fig. 3b shows a fragment of the grid photograph through an 8-mm-high water layer on whose surface waves were excited. The subwoofer excitation frequency is 37 Hz, and the relative pumping amplitude of the vibroplatform is $A = 6$. As is seen, the distance between spots changes as a function of their position in the figure, thus corresponding to a displacement of the point image because of the refraction at the vibrating liquid surface. The algorithm for processing photographs is presented below:

(1) A photograph is reduced to a two-color variant (each pixel on the photograph is either black or white, without color gradations) via changes in the photograph contrast and brightness.

(2) Each spot on the photograph has a size of ~10–20 pixels. The coordinates of the geometrical center of each spot are determined. Subsequently, these coordinates are considered to be the coordinates of this spot.

(3) The correspondence of spots on the photograph to spots on the grid is established. For this purpose, 2D indexation of spots on the photograph is introduced. Because it is known (Fig. 3a) that the initial grid has a square structure and the relative image displacement of spots on the photograph, which results from the excited vibrations on the water surface, is much smaller than the distance between neighboring spots (Fig. 3b), the indexation algorithm reduces to a search for neighboring spots near each spot. The neighboring spots are located within certain angular sectors and a certain range of distances.

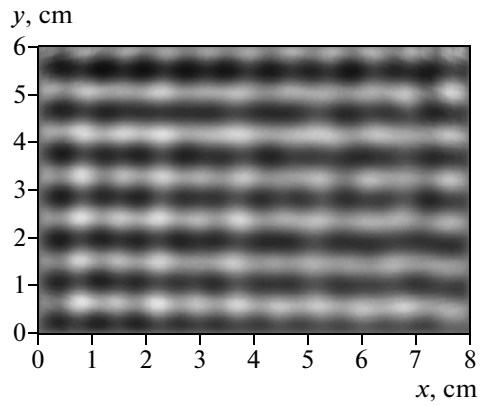

Fig. 4. Example of the reconstructed shape of the vibrating liquid surface.

(4) Subsequently, the coordinates of spots on two photographs are compared—through the vibrating and quiet (unexcited) liquid surface. For each pair of spots on the photographs that correspond to one spot on the grid, the displacement, i.e., the difference of their coordinates $\Delta x_{i,j}$ and $\Delta y_{i,j}$, is determined.

(5) In order to numerically integrate equation (4), the following boundary conditions are introduced:

$$h(0, y) = h(x_{\max}, y) = h(x, 0) = h(x, y_{\max}) = 0. \quad (5)$$

Note that such boundary conditions are physically correct only when the dimensions of the grid, which is placed on the cell bottom, coincide with the dimensions of the cell,

(6) The numerical integration of (4) with boundary conditions (5) yields the function $h(x, y)$ that reproduces the shape of the liquid surface. Figure 4 shows an example of the reconstructed shape of the vibrating liquid surface. The axes in the figure are directed along the walls of the rectangular cell; the X axis is oriented along the long side of the cell. The color intensity in the figure corresponds to the height of the liquid surface: the color darkens, as the surface level decreases.

(7) To calculate the energy distribution over wave vectors, we apply a 2D Fourier transform to the function $h(x, y)$ multiplied by the Bleckman window function.

(8) To reduce the quantization noise in one experimental run, we processed a set of 20 grid photographs that were taken under identical experimental conditions and then averaged the obtained spectra over this set. When processing these photographs, it should be also considered that the liquid-surface region through which rays from the grid pass is smaller than the geometric dimensions of the grid because of the finite distance between the grid and camera.

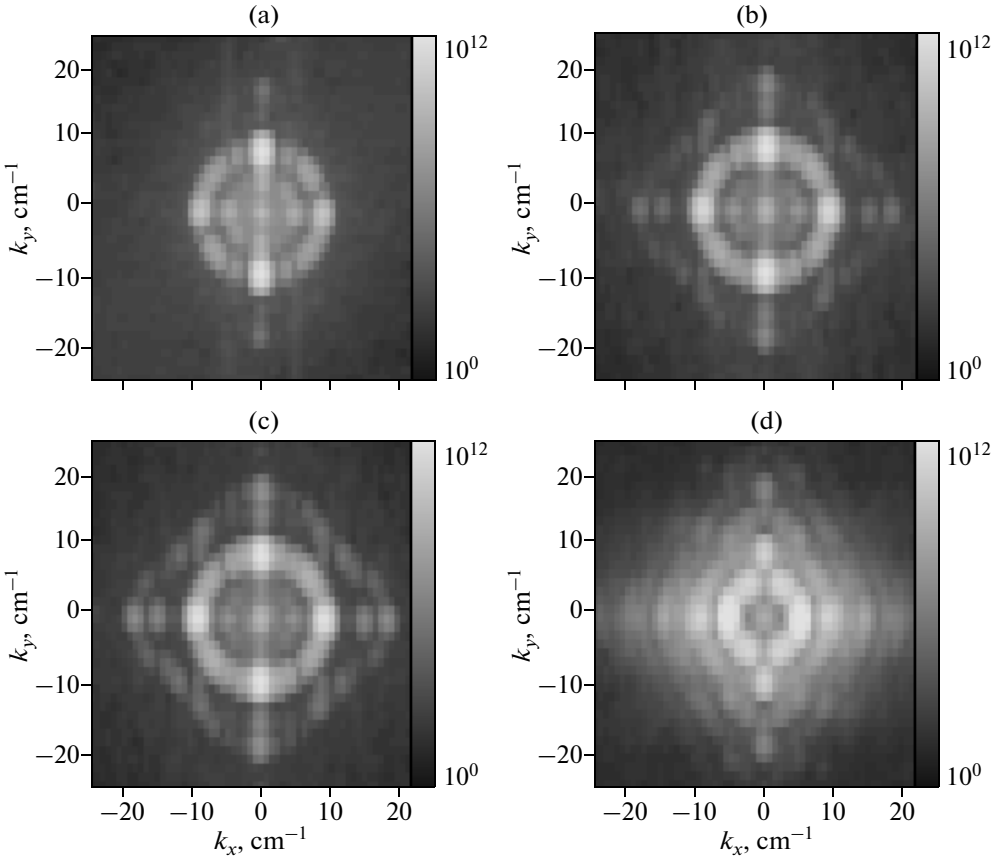

Fig. 5. Energy distribution over wave vectors for relative pumping amplitudes $A = 1.5$ (a), 4.5 (b), 7.5 (c), and 9.5 (d).

EXPERIMENTAL RESULTS

The results are presented for an experiment that was performed in water inside a glass cell with inner dimensions of 90 × 70 mm. The size of the grid that was under the cell bottom was 80 × 60 mm, the white point was 50 × 50 μm in size, and the grid was square with a pitch of 250 μm. The corresponding number of points in the grid was 320 × 200. Before measurements, the cell was filled with distilled water; the water-layer depth was 8–10 mm.

Figure 5 shows the results of calculating the energy distribution over wave vectors upon application of a monochromatic signal at the frequency $\nu = 38$ Hz with different pumping amplitudes to the vibroplatform. The wave vectors k_x and k_y (k_x and k_y: are the projections of the vector **k**) are plotted along the axes; the color brightness determines the energy intensity in the wave. It should be reminded that the X axis in this and subsequent plots corresponds to the direction along the long side of the rectangular cell. In this experiment, the spectra were averaged (see item (8) in the processing algorithm).

Figure 5a presents the results of calculating the energy distribution over wave vectors for a relative pumping amplitude of $A = 1.5$. The figure depicts a circle corresponding to $k = \text{const}$, on which there are four bright spots that are peaks corresponding to two distinguished directions of the rectangular cell. The wave vectors with a relatively small amplitude that are within the circle correspond to the noise pumping as a result of a setup jutter, which is caused by building vibrations.

Figure 5b illustrates the change in the shape of the energy distribution over wave vectors upon a threefold increase in the pumping amplitude to $A = 4.5$. The figure shows the appearance of peaks, which correspond to the second harmonic, in the energy distribution over wave vectors. Note that the shape of the energy distribution over wave vectors for the second harmonic is closer to a rectangular profile, as opposed to the first harmonic.

In Fig. 5c, the relative pumping amplitude is increased to $A = 7.5$, and the peak intensity is also appreciably higher.

In Fig. 5d, the relative pumping amplitude is $A = 9.5$. In addition to the distribution shown in Fig. 5c, a bright circle with a smaller diameter appears here, which corresponds to intense liquid vibrations at the half-frequency of pumping. Thus, we observe a manifestation of a Faraday instability during the parametric procedure of surface-wave excitation.

The dispersion law for surface waves is described by two terms, gravitational and capillary:

$$\omega^2 = gk + \frac{\sigma}{\rho}k^3, \quad (6)$$

where ω is the cyclic frequency of vibrations, k is the wave-vector magnitude, g is the acceleration of gravity, σ is the surface tension coefficient, and ρ is the liquid density.

The problem of the influence of the liquid-layer depth on the dispersion law of gravitational waves was solved in [7]. Using this estimate, it can be expected that for waves in the measured frequency range, the influence of the cell bottom on surface waves is negligibly weak. This assumption is also confirmed by the experimental data.

The gravitational component can be disregarded at large k and correspondingly high frequencies. Note that the capillary term becomes equal to the gravitational term at a frequency of 15 Hz.

In order to reconstruct the dispersion law for capillary waves, i.e., the dependence $\omega(k)$, we performed a run of measurements at frequencies of 10–400 Hz with a step of 10 Hz. In this experiment, a 65-mm-diameter cylindrical cell and a grid with dimensions of 48 × 30 mm were used. The number of points on the grid was 321 × 201. The depth of the water was 10 mm. As the frequency increased, the pumping amplitude of a sinusoidal signal that arrived at the subwoofer input increased as well. The energy distribution over wave vectors was plotted for each pumping frequency. In each distribution, the value of k that corresponded to the pumping frequency was chosen. The obtained values of k were used to construct the curve for the dispersion law $\nu(k)$ shown in Fig. 6 (dots). This plot also shows a solid curve that corresponds to the dependence described by the formula

$$\nu = \frac{1}{2\pi}\left(gk + \left(\frac{\sigma}{\rho}\right)k^3\right)^{1/2}. \quad (7)$$

This calculated curve was constructed using the following values: $\sigma = 72$ dyne/cm, $\rho = 1$ g/cm^3, and $g = 981$ cm/s^2.

The tabulated value of the surface-tension coefficient for distilled water is $\sigma_T = 72$ dyne/cm [6, 8].

CONCLUSIONS

The proposed technique can be used for measuring the dispersion dependences for surface waves in cells of different geometries, studying nonisotropic vibrations on the surface of a liquid and the influence of surface-active layers on the properties of a liquid surface, as well as studying nonlinear effects on surfaces.

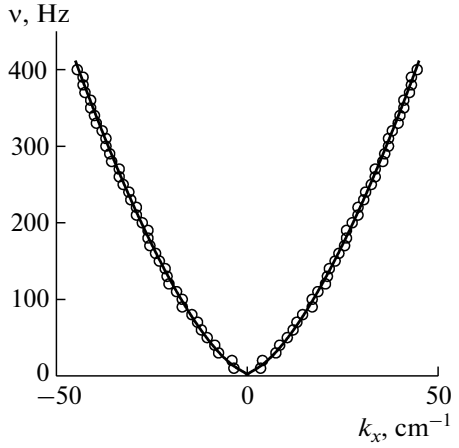

Fig. 6. Wave dispersion law on the water surface. The smooth curve corresponds to the theoretical law with the surface-tension coefficient $\sigma_T = 72$ dyne/cm.

We plan to upgrade the system for studying turbulent cascades on liquid surfaces.

ACKNOWLEDGMENTS

We are grateful to A.V. Lokhov for his help in preparing this experiment and L.P. Mezhov-Deglin and L.V. Abdurakhimov for useful discussions.

This study was supported in part by the Council for Grants of the President of the Russian Federation for Support of Leading Schools (project no. NSh-6453.2012.2).

REFERENCES

1. Brazhnikov, M.Yu., Levchenko, A.A., and Mezhov-Deglin, L.P., *Instrum. Exp. Tekh.*, 2002, vol. 45, no. 6, p. 758.
2. Abdurakhimov, L.V., Brazhnikov, M.Yu., Remizov, I.A., and Levchenko, A.A., *JETP Lett.*, 2010, vol. 91, no. 6, p. 291.
3. Falcon, E., Laroche, C., and Fauve, S., *Phys. Rev. Lett.*, 2007, vol. 98, no. 9, p. 094503.
4. Wright, W.B., Budakian, R., and Putterman, S.J., *Phys. Rev. Lett.*, 1996, vol. 76, no. 24, p. 4528.
5. Henry, E., Alstrom, P., and Levinsen, M.T., *Europhys. Lett.*, 2000, vol. 52, no. 1, p. 27.
6. Fujimura, Y. and Iino, M., *J. Appl. Phys.,* 2008, vol. 103, no. 12, p. 124903.
7. Landau, L.D. and Lifshits, E.M., *Teoreticheskaya fizika. T. 6. Gidrodinamika* (Theoretical Physics, vol. 6, Fluid Mechanics), London: Pergamon, 1987.
8. Li, Ch., Chen, L., and Ren, Zh., *Rev. Sci. Instrum.*, 2012, vol. 83, no. 4, p. 043906.

Translated by A. Seferov